240 (2024) 213038

Contents lists available at ScienceDirect

Geoenergy Science and Engineering

journal homepage: www.sciencedirect.com/journal/geoenergy-science-and-engineering

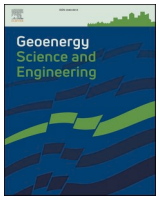

Thermal steam treatment effect of metallic sodium nanoparticles for high-carbon, low permeability Domanic rocks

Liliya Kh Galiakhmetova [a], Aydar A. Kayumov [a], Vladimir E. Katnov [a,**], Mohammed A. Khelkhal [a,***], Rezeda E. Mukhamatdinova [a], Sofya A. Trubitsina [a], Nafis A. Nazimov [b], Alexey V. Vakhin [a,*]

[a] Institute of Geology and Oil & Gas Technologies, Kazan Federal University, Kazan, 420008, Russia
[b] PJSC «TATNEFT», Lenin St., 75, Almetyevsk, 423450, Russia

ARTICLE INFO

Keywords:
Domanic deposits
Organic matter
Kerogen
Sodium nanoparticles
Hydrothermal treatment
Bitumoid
Desulfurization
Hydration
Hydrogenolysis

ABSTRACT

In a study aimed at exploring novel methods for enhancing hydrocarbon extraction from shale reservoirs, we conducted an experimental study to model the effects of thermal steam treatment on high-carbon, low-permeability Domanic shale in the presence of sodium metal nanoparticles. We characterized the mineral composition of the rock samples and evaluated the yield and quality of extracted hydrocarbons before and after treatment. Our results demonstrated an increase in extract yield with increasing treatment temperature. Notably, we observed a significantly augmented effect when we introduced sodium nanoparticles into the reaction system, enabling a 100 °C reduction in treatment temperature while maintaining comparable capabilities for extracting organic matter. It was found that the experimental products exhibited enrichment in saturated hydrocarbons, coupled with a decrease in resinous-asphaltenic substances. Within the saturated fraction, we observed a shift towards lighter alkanes and cycloalkanes (C_{12}–C_{14}). Moreover, it has been found that the highest yield of low molecular weight liquid hydrocarbons is acheived in the experiment involving sodium nanoparticles at 250 °C. Upon further increasing the temperature to 300 °C, we noted a decline in liquid hydrocarbon content, accompanied by an increase in gaseous hydrocarbons (C_1–C_4). Besides, thermal steam treatment substantially reduced the proportion of sulfur-containing aromatic compounds, such as alkylbenzothiophenes, dibenzo- and naphthothiophenes, in the aromatic fraction. The addition of sodium nanoparticles facilitated near-complete desulfurization of this fraction. Moreover, we observed a significant reduction in the total sulfur content of the extracted organic matter. Hydrothermal treatment in the presence of nanoparticles induced transformations in the kerogen structure and structural and phase changes in the mineral components of the shale.

1. Introduction

Despite the ongoing transition towards renewable energy sources, oil and natural gas remain the principal energy resources in the modern era (Zou et al., 2016). While nations worldwide are exerting significant efforts to develop sustainable alternatives, petroleum products are likely to prevail as the predominant fuel for transportation, agricultural machinery, military equipment, and a crucial feedstock for the petrochemical industry in the foreseeable future (Fallis, 2013). The continued exploitation of crude oil will potentially serve as a vital catalyst for economic growth and societal development in industrialized countries over an extended period (Fallis, 2013).

For the last decades, a keen interest has emerged in developing technologies that enable the economically viable exploration of unconventional hydrocarbon resources (Foda, 2015). This interest stems from the depletion of conventional oil reservoirs (Aguilera et al., 2009). Particular attention has been directed towards shale oil and gas formations (source rocks) (Aadnøy and Looyeh, 2019), fueled by the substantial volume of potential resources this type of feedstock presents.

Within the Republic of Tatarstan, the oil-bearing shale formations are represented by the Domanic complex, which was formed under conditions of uncompensated depressions and troughs from the early

* Corresponding author.
** Corresponding author.
*** Corresponding author.
E-mail addresses: vkatnov@yandex.ru (V.E. Katnov), amine.khelkhal@gmail.com (M.A. Khelkhal), vahin-a_v@mail.ru (A.V. Vakhin).

https://doi.org/10.1016/j.geoen.2024.213038
Received 22 April 2024; Received in revised form 8 June 2024; Accepted 8 June 2024
Available online 16 June 2024

Semiluki to the late Tournai periods (Morozov et al., 2022). The Domanic formations, characterized by a high concentration of organic matter, are considered source rocks and consist of silicified limestones, dolomites, and marlstones, exhibiting varying degrees of cavernosity and fracturing (Liang et al., 2020). A unique feature of these formations is the presence of kerogen, a substance possessing oil-generating potential that can transform into mobile hydrocarbons under specific conditions (Kravchenko et al., 2018; Vandenbroucke, 2003).

The intricate structure of the formations and the coexistence of hydrocarbons in both free and bound states within the rock (Gabrielsen, 2010) complicates the mechanism of exploiting the Domanic deposits, necessitating the search for novel and efficient development technologies. Existing horizontal drilling and hydraulic fracturing techniques allow for the extraction of only light oil – the analog of "tight oil" in the United States (Ibatullin, 2017). However, the paramount objective in the development of this class of reservoirs is to harness their potential reserves concealed within the kerogen (Kravchenko et al., 2018; Agrawal and Sharma, 2018). In nature, the transformation of kerogen into synthetic oil occurs spontaneously over geological timescales (millions of years) due to the gradual increase in pressure and temperature during sedimentation (Kalmykov et al., 2017). To obtain hydrocarbons from the organic matter of kerogen within realistic timescales, an additional external impact on the kerogen-bearing rock is required (Karpov et al., 1998). Recent years have witnessed a surge in research dedicated to the conversion of kerogen's organic matter into mobile hydrocarbons through thermal treatment (Kalmykov et al., 2017; Onishchenko et al., 2019; Vakhin et al., 2024; Kayukova et al., 2016; Bychkov et al., 2015; Behar et al., 2010; Liang et al., 2015; Zhang et al., 2014). In the pursuit of optimal technologies, complex methods, including thermochemical approaches (Galukhin et al., 2019; Al-Mishaal et al., 2022; Tajik et al., 2023; Kravchenko et al., 2016) employing various catalysts, have been explored. These catalysts have already demonstrated their efficacy in enhancing the production of another unconventional hydrocarbon resource – heavy, high-viscosity oils. For instance, Mikhailova et al. (2020) investigated the influence of oil-soluble metal carboxylates of Fe, Co, and Cu on the properties and hydrocarbon generation from the carbonate-siliceous rocks of the Domanic deposits. Experimental evidence revealed an increase in the yield of extracts from the rock formations in the presence of a metallic catalyst within the reaction system. Additionally, several studies have been conducted on the effects of sub- and supercritical water (Nasyrova et al., 2020a, 2020b, 2021), CO_2 (Kayukova et al., 2020), and 1-propanol (Nasyrova et al., 2022) on the transformation of organic matter in the Domanic formations. Kayukova et al. (2019) highlighted the potential use of iron-containing catalysts to intensify the oil extraction process from the Domanic formations, with natural minerals such as pyrite and hematite serving as precursors for these substances. Nevertheless, several obstacles remain, including low coverage of catalyst exposure due to the extremely low permeability of the rocks, heterogeneity of the deposits across the area and section, and high costs, which limit the feasibility of large-scale application of these technologies.

The implementation of nanoparticles is being actively explored by many researchers as a potential solution to the majority of challenges associated with enhanced oil recovery methods (Sun et al., 2017; Shayan Nasr et al., 2021). This perspective is attributed to their diminutive size relative to pore channel dimensions, enabling them to penetrate the rock formation with minimal impact on permeability (Alomair et al., 2014). According to Alomai et al. (Alomair et al., 2014), the utilization of nanoparticles ranging from 1 to 100 nm in size presents opportunities for the extraction of oil from low-permeability reservoir pore spaces of approximately 5–50 μm. In addition to their ultra-small dimensions, nanoparticles possess another advantageous attribute: an exceptionally high surface area-to-volume ratio, resulting in a substantial proportion of surface atoms (Zhang and Liu, 2001), which enhances their reactivity. Furthermore, the majority of the nanoparticles widely employed in chemical enhanced oil recovery methods are considered environmentally benign materials compared to chemical substances. For instance, a significant portion of silica (SiO_2) nanoparticles is composed of silicon dioxide, which constitutes a principal component of sandstone (Sun et al., 2017), while alumina (Al_2O_3) nanoparticles are a constituent of clays. In their work (Maghzi et al., 2012) Maghzi et al. conducted investigations into the influence of nanofluids on rock wettability and uncovered the ability of SiO_2 nanoparticles to alter the wettability of shales from oil-wet to water-wet. Other studies (Sitnov et al., 2019; Aliev et al., 2021; Lakhova et al., 2017) have reported that the utilization of nanodispersed transition metal-based catalysts leads to a reduction in the viscosity of the extracted oil, an increase in the content of saturated hydrocarbons, and an enhanced yield of lighter fractions.

Synthesizing the findings from research in this domain, it is evident that the quest for effective technologies to develop the high-carbon, low-permeability Domanic deposits and their analogs has never been more pressing. Devising productive technologies necessitates a multifaceted approach, aimed at realizing the oil-generating potential of the Domanic formations while simultaneously enhancing the reservoir's porosity and permeability characteristics. This realization prompted us to conduct investigations focused on improving the oil recovery from Domanic rocks through the application of an organodispersion of metallic sodium nanoparticles, which demonstrated promising results in our previous study on the upgrading of heavy oil from the Ashalcha field (Katnov et al., 2023). We hypothesize that the dispersed metallic sodium, injected via hydraulic fracturing technology, will interact with the formation water, liberating gaseous hydrogen and heat through the following reaction:

$$2Na + 2H_2O \rightarrow 2NaOH + H_2^{\uparrow} + 279.2\ kJ$$

The highly mobile active hydrogen, owing to its minute size, can readily penetrate the pores of the reservoir formation. Additionally, the temperature rise to 60 °C or higher, generated by this exothermic chemical reaction, increases the gas volume within the pores and enhances the fluidity of all oil fractions, particularly the heavier components. Concurrently, at temperatures of 60 °C and above, the transformation of kerogen into the liquid phase commences (60 °C marks the onset of the oil window), accompanied by a substantial reduction in the viscosity of paraffins and asphaltenes (35–45 mPa s and 48–55 mPa s, respectively, at 60 °C). Parallelly, the NaOH ions lower the interfacial tension through the activation of aromatic compounds, facilitating their hydrogenation. For paraffins and asphaltenes (heavy oil fractions), this process may proceed via sulfide bridges, leading to a reduction in their molecular weight, akin to the mechanism observed in the presence of a copper-containing catalyst (Aliev et al., 2021), as illustrated in Fig. 1.

A number of studies have demonstrated the upgrading of heavy oil in the presence of sodium ions (Gray, 2019; Kosachev et al., 2022) through the removal of bound sulfur, facilitated by the interaction of sodium ions with mercaptans present in bitumen, which undergo transformation into mercaptides.

Upon contact between the alkali and oil, a reaction occurs with the organic acids contained in the oil (primarily naphthenic acids), mainly involving carboxyl groups, resulting in the formation of surface-active substances that contribute to the reduction of interfacial tension at the oil-water phase boundary and enhance the water wettability of the rock.

As a consequence of the aforementioned processes, the pores become liberated from the heavy oil fractions, leading to improved porosity and permeability characteristics of the productive formation. Additionally, chemical conversion and viscosity reduction of the heavy oil are achieved, the culminating effect of which is an increase in oil recovery.

The objective of the present work is to evaluate the influence of an organodispersion of metallic sodium nanoparticles on the mineral composition of rocks and the transformation of the organic matter (OM) contained therein during hydrothermal treatment, using the high-carbon, low-permeability Domanic deposits as a case study.

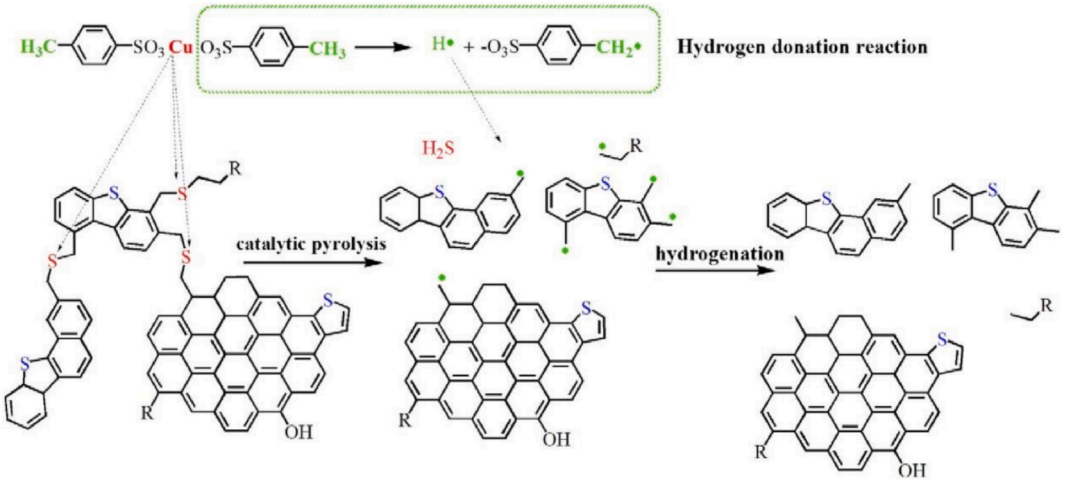

Fig. 1. Mechanism of destruction of C–S bonds (Aliev et al., 2021).

2. Experimental section

The object of investigation was rock samples obtained from the Domanic deposits of the Ashalcha field, located on the western slope of the South Tatar Arch, within the Cheremshano-Yamashinsky structural zone of the second order. The rock samples were studied before and after hydrothermal treatment at varying temperatures, both in the presence and absence of sodium nanodispersion.

The preparation of the nanosuspension employed a method described in (Tang et al., 2018), wherein metallic sodium was cut into pieces and transferred into a liquid paraffin medium according to the scheme illustrated in Fig. 2. Subsequently, this mixture was heated to the melting point of sodium, and once the sodium pieces melted into spherical, glistening globules, dispersion was carried out in an UP200Ht ultrasonic generator at an amplitude of 70% and the corresponding power.

The resulting suspension with a grayish-purple hue was subjected to cooling by immersing the chemical beaker into a larger container filled with cold water. The obtained sodium nanosuspension was analyzed using dynamic light scattering with a Brookhaven ZetaPlus nanoparticle analyzer.

The thermobaric treatment of the Domanic rock was conducted in a ChemRe SYStem VR-201 reactor autoclave (300 mL volume) coupled with a Khromatek Kristall 5000 gas chromatograph. The initial pressure was set at 10–10.2 bar, with target temperatures of 150, 200, 250, and 300 °C, and a holding time of 24 h. The model system comprised a mixture of 100 g of Domanic rock crushed to a 0.25 mm fraction and 25 g of a 20% sodium suspension in Nefras C4-155/205 (20 g of Nefras C4-155/205 in the case of the control sample). To prevent direct contact with water, a glass container filled with distilled water in a rock-to-water mass ratio of 100:10 was immersed in the center of the reactor (Fig. 3).

Upon completion of the experiment, the gaseous phase was removed from the autoclave after determining the component composition, followed by the unloading of the rock for subsequent analysis using a suite of instrumental methods.

To conduct the analysis, a gas phase sample was taken from the autoclave through a gas outlet via a special gas line leading to the chromatograph. During the chromatographic process, the gas sample was separated on a packed column (Hayesep Q, 1.5 m × 2 mm, 80/100 mesh) into hydrogen sulfide and carbon dioxide, which were then detected using a TCD-1 detector. On the NaX column (2 m × 3 mm, 60/80 mesh), hydrogen, oxygen, and nitrogen were separated and detected using a TCD-2 detector. The separation of hydrocarbon gases was performed on a capillary column (CR-1 PONA, 100 m × 0.25 mm × 0.5 μm) and detected using a flame ionization detector. The temperature program was: (35 °C; 13 min) → (10 °C/min; 45 °C; 15 min) → (1 °C/min; 60 °C; 15 min) → (2 °C/min; 240 °C; 41 min). Helium was used as the carrier gas, with a pressure of 323 kPa at the inlet of the capillary column and a flow rate of 15 mL/min through the packed columns. The obtained analysis results were processed using the "Chromatec Analytic 3.1″ software (Chromatec).

Bitumoids were extracted from the rock before and after the experiments in a Soxhlet apparatus, employing a solvent mixture of chloroform, benzene, and isopropyl alcohol in a 1:1:1 ratio, offering varying degrees of polarity.

The fractional composition of the extracts was determined by the SARA analysis method in accordance with ASTM D2007 recommendations. Asphaltenes were precipitated by the addition of a 40-fold excess of the aliphatic solvent hexane. The maltenes were fractionated using a glass chromatographic column packed with aluminum oxide calcined at 450 °C. Separation into saturated hydrocarbon, aromatic hydrocarbon, and resin fractions was achieved through sequential elution with appropriate solvents. Saturated hydrocarbons were dissolved in 220 mL of n-hexane, aromatic hydrocarbons in 200 mL of toluene, and resins

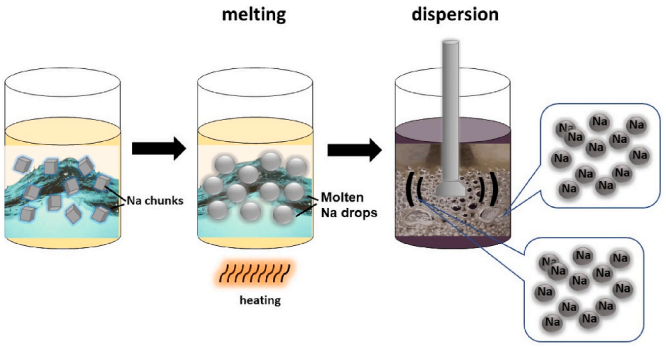

Fig. 2. Scheme for obtaining sodium nanodispersion.

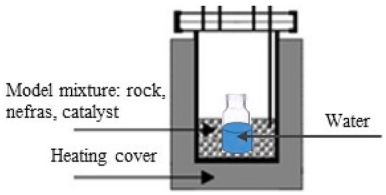

Fig. 3. Diagram of contacting reagent loading.

were washed off the adsorbent with a mixture of 150 mL of toluene and 50 mL of isopropanol.

The analysis of the group and individual compositions of saturated and aromatic hydrocarbons was performed using a GC-MS system comprising a Chromatech-Crystal 5000 gas chromatograph coupled with an ICQ mass-selective detector (USA). The obtained results were processed using the Xcalibur software. A 30 m × 0.25 mm capillary column CR-5ms was employed for the analysis. Helium was used as the carrier gas at a flow rate of 1 mL/min and a temperature of 310 °C. The optimized oven temperature program began with an initial ramp from 100 to 150 °C at a rate of 3 °C/min, followed by a ramp from 150 to 300 °C at a rate of 12 °C/min, and a subsequent isothermal hold until the end of the analysis. The components of the saturated and aromatic fractions were identified using the NIST mass spectral library and literature sources (Gordadze et al., 2010).

The structural group composition of resins and asphaltenes was determined by Fourier-transform infrared (FTIR) spectroscopy using a Spectrum two PERKIN ELMER spectrometer equipped with a UATR (Single Reflection Diamond) accessory for the Spectrum Two. The dried asphaltenes and resins were placed on the accessory and pressed using a manual press to obtain maximum absorption, after which the measurements were performed. The measurement range was 4000-450 cm^{-1} with a resolution of 4 cm^{-1}.

The sulfur content in the bitumoids was determined using an energy-dispersive X-ray fluorescence spectrometer, Spectroscan SUL. This analyzer is capable of measuring ultra-low sulfur concentrations from 0.0003 to 5 wt% and is designed for determining the mass fraction of sulfur in crude oil and petroleum products in accordance with GOST R 51947-2002, GOST R EN ISO 20847-2010, and GOST 305-82. The instrument was calibrated using a series of standard mineral oil samples, similar in physicochemical properties to diesel fractions, with known sulfur contents ranging from 0.00036 to 0.1 wt%. The bitumoid samples were initially dissolved in diesel with a known sulfur content of 0.5–1%, and the resulting mixture was analyzed for sulfur content, after which the data were recalculated for the original bitumoid.

The mineral composition of the original rock and the rock subjected to steam-thermal treatment in the presence and absence of sodium nanodispersion was investigated by X-ray powder diffraction (XRD) using a Shimadzu XRD-7000S diffractometer equipped with a nickel monochromator on the diffracting beam, a step size of 0.0008 A^{-1}, and a single point exposure time of 3 s; and a D2 PHaser Bruker diffractometer with CuKα radiation (λ = 1.54060 nm). The processing of diffraction spectra and identification of the crystalline phases present were performed using the original interactive computer system EVA (version 4.0), designed for the study of sedimentary rocks and soils, and incorporating specialized ICDD-2010 databases.

3. Results and discussion

3.1. Influence of metallic sodium nanoparticles on organic matter transformation during hydrothermal treatment of high-carbon rocks

During thermobaric exposure of the Domanic rock, an increase in the yield of extractable bitumoids from the core is observed. As evident from the results presented in Fig. 4, in the control experiments, an over threefold increase in extract yield is achieved at a temperature of 300 °C with increasing temperature. In the presence of sodium nanoparticles in the reaction system, the increment is even more substantial – at an experiment temperature of 150 °C, the extract yield doubles, whereas a similar increase in bituminosity is observed in the control sample at 250 °C. Thus, the application of metallic sodium nanoparticles offers the advantage of reducing the steam-thermal treatment temperature by 100 °C while maintaining a comparable capacity for organic matter extraction, undoubtedly reducing the economic costs associated with heating the heat transfer medium.

The results of the conducted experiments indicate the realization of

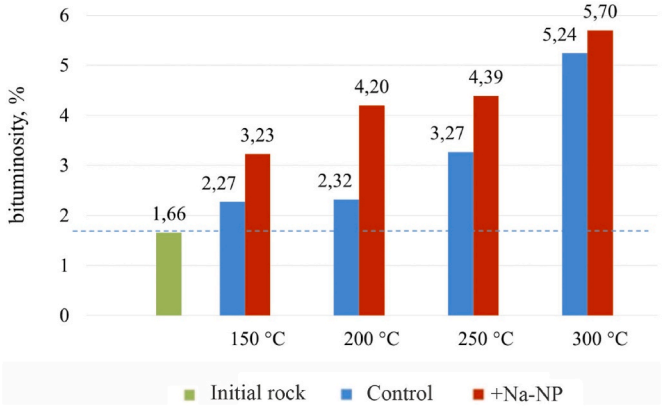

Fig. 4. Yield of extracts before and after experiments.

the generation potential of the Domanic kerogen during steam-thermal treatment, as evidenced by the formation of a significant amount of the so-called "synthetic oil" (Kalmykov et al., 2017). The addition of a sodium nanosuspension during steam-thermal treatment may lead to an increase in the oil recovery from the Domanic deposits, as our previous studies (Katnov et al., 2023) on the interaction between the Ashalcha field oil and a sodium organodispersion demonstrated the possibility of its upgrading, viscosity reduction, and hydrogen sulfide capture.

Hydrothermal treatment of the rock is accompanied by the release of hydrocarbon (CH_4, C_2H_4, C_2H_6, C_3H_8, etc.) and inorganic gases (H_2, O_2, N_2, CO, and CO_2). As can be seen from the data presented in Table 1, the yield of hydrocarbon gases increases with increasing steam-thermal treatment temperature: in the control samples from 0.02 to 2.87 wt%, and in the samples with metallic sodium from 0.31 to 4.17 wt%. Notably, in the control sample, a substantial change in gas yield with a value of 2.87 wt% is observed only at 300 °C, as clearly illustrated in Figure A1 (Appendix 1). Among the inorganic gases, the trends are less unambiguous. In the control samples, the concentration of carbon dioxide, hydrogen sulfide, and hydrogen increases with increasing treatment temperature, while the oxygen content decreases. The application of sodium nanoparticles during steam-thermal treatment promotes an increase in hydrogen and oxygen content, and a reduction in the proportion of carbon dioxide and hydrogen sulfide in the evolved gases. The hydrothermal treatment was conducted in a gaseous nitrogen environment, accounting for its maximum trace in the gas samples.

The formation of H_2S in the experiments is indicative of destructive processes occurring along the aliphatic S–S and S–C bonds of heteroatomic organic matter compounds. Additionally, in the experiments involving metallic sodium nanoparticles, pyrite, which undergoes transformation into hematite during the treatment process as established by the X-ray diffraction analysis data presented below, may serve as an additional source of sulfur for H_2S formation. In the control samples, with increasing hydrocarbon gas concentration, the oxygen content decreases, and the proportion of carbon dioxide increases. The majority of carbon dioxide, as suggested by many researchers (Zhao et al., 2012; Clark et al., 1983; Kruse and Dinjus, 2007), is released through the decarboxylation of carbonyl-containing compounds in bitumen (aldehydes, ketones, and esters (Lewan, 1997; Tumanyan et al., 2015)) via the water-gas shift reaction under aquathermolysis conditions: $CO + H_2O \rightarrow CO_2 + H_2$. Additionally, the oxidative degradation of hydrocarbons is indicated by the reduction of O_2 in the composition of the released gases. As the temperature increases, more organic matter is involved in these processes, resulting in a higher proportion of carbon dioxide and hydrogen in the gas cap in the control samples.

The interaction of sodium nanoparticles with water generates a large amount of hydrogen, leading to a shift in the direction of redox reactions, as indicated by the increased concentration of oxygen in the released gases. In experiments with metallic sodium, which creates an

Table 1
Gas composition of the experimental products.

Experiment Temperature	Content, wt. %									
	C_1	C_2	C_3	C_4	H_2	O_2	N_2	CO_2	H_2S	Sum
150 °C, control	0.002	0.002	0.007	0.013	0.000	0.688	98.061	0.969	0.008	100
200 °C, control	0.007	0.005	0.015	0.027	0.000	0.139	94.285	5.074	0.015	100
250 °C, control	0.026	0.019	0.028	0.033	0.014	0.141	87.334	11.872	0.107	100
300 °C, control	0.796	0.824	0.769	0.482	0.151	0.083	81.447	13.633	1.354	100
150 °C, +Na-NP	0.187	0.061	0.033	0.029	2.635	1.012	95.817	0.006	0.015	100
200 °C, +Na-NP	0.468	0.154	0.069	0.038	2.762	1.067	95.321	0.013	0.017	100
250 °C, +Na-NP	1.332	0.454	0.145	0.091	2.699	0.932	93.929	0.013	0.014	100
300 °C, +Na-NP	2.802	0.842	0.337	0.185	2.730	0.506	92.665	0.012	0.012	100

C_1- C_4-alkanes and alkenes with the corresponding number of carbon atoms.

alkaline environment when reacting with water, the water-gas shift reaction does not proceed towards the formation of molecular hydrogen (Ross and Nguyen, 1983). Instead, CO predominantly reacts with the alkali to form formates: CO + NaOH → HCOONa. These formates then participate in hydrogenation and hydrogenolysis reactions (illustrated below with compound X):

$$X + HCOONa \rightarrow XH^{-}Na^{+} + CO_2$$

$$XH^{-}Na^{+} + H_2O \rightarrow NaOH + XH_2$$

In this case, an ionic mechanism of hydrogenation and hydrogenolysis is realized, i.e., the breaking of carbon-heteroatom bonds with the addition of a hydride ion and the subsequent regeneration of the hydroxide ion. Additionally, the sodium hydroxide produced from the interaction of sodium nanoparticles with water reacts with hydrogen sulfide and carbon dioxide, forming water-soluble sodium sulfide and sodium carbonate, respectively, thereby minimizing their presence in samples containing nanoparticles.

The formation of C_1–C_4 hydrocarbon gases indicates the occurrence of destructive processes involving the cleavage of C–C bonds. At a temperature of 300 °C, the amount of evolved gaseous hydrocarbons increases substantially, and further temperature elevation may lead to a decrease in the proportion of liquid saturated hydrocarbon fractions due to alkane destruction and an increase in the proportion of gaseous products with chain lengths of C_1–C_4. This finding is corroborated by the work of Bychkov et al. (2015), who, while investigating the possibility of obtaining hydrocarbon fluids from the Bazhenov Formation rocks during hydrothermal treatment, established that increasing the treatment temperature enhances the proportion of gaseous hydrocarbons, and at temperatures above 450 °C, all extracted organic matter is converted into gaseous products. In this case, no oil fractions were present, and the kerogen was substantially graphitized.

Analysis of the group composition of the extracts reveals a general trend – with increasing treatment temperature, the proportion of saturated hydrocarbons increases while the resin-asphaltenic substances (RAS) decrease (Table 2), indicating the predominance of hydrogenation, hydrogenolysis, and isomerization reactions over condensation reactions.

Table 2
Group composition of bitumen before and after experiments.

Experiment Temperature	Extracts Group composition, wt. %			
	Saturates	Aromatics	Resins	Asphaltenes
Initial sample				
	10.36	21.69	46.95	21.00
Post thermal steam exposure				
150 °C	24.14	13.45	42.04	20.37
200 °C	19.76	14.06	33.72	32.46
250 °C	33.12	16.94	18.25	31.69
300 °C	40.81	17.42	22.71	19.06
Post thermal steam exposure in the presence of Na nanoparticles				
150 °C	47.48	13.36	17.44	21.72
200 °C	43.97	10.54	12.87	32.61
250 °C	45.21	12.71	13.88	28.20
300 °C	39.89	14.23	18.61	27.28

In the control sample, the proportion of saturated and aromatic hydrocarbons increases almost linearly with increasing temperature. Meanwhile, the addition of a sodium organodispersion allows for the observation of such positive changes even at the minimum treatment temperature. However, further increasing the treatment temperature to 300 °C alters the pattern of organic matter transformation, leading to a reduction in the proportion of saturated hydrocarbons in the extract composition, which, as noted above, indicates their transition to the gaseous state.

It is noteworthy that when comparing the fractional composition of the control sample and the sample with sodium nanoparticles, which exhibit similar bituminosity values (Fig. 4) at temperatures of 250 and 150 °C, respectively, differences in the fractional ratios are observed. These differences are expressed as a simultaneous increase in the saturated hydrocarbon fraction by 14 wt% and a decrease in the RAS fraction by 10 wt% in the presence of sodium nanoparticles compared to the control sample. When conducting a comparative analysis of the extract fractional composition, it is essential to consider that the synthetic oil formed during the hydrothermal treatment comprises both products of the original oil transformation and oil generated from kerogen decomposition. Thus, the increase in the content of lighter fractions in the experiment products may be attributed, firstly, to the destruction of resins from the original oil, as indicated by the decrease in their content in the group composition of the extracts, and secondly, to kerogen decomposition and the simultaneous transformation of high-molecular-weight compounds into low-molecular-weight ones. The increase in the asphaltene content after the experiments is evidently due to kerogen destruction.

In addition to quantity, it is crucial to evaluate the composition of the hydrocarbon compounds obtained during hydrothermal treatment. Fig. 5 presents the chromatograms of the saturated fraction of the original bitumoid and the experiment products under various conditions.

In the original chromatogram, peaks corresponding to both normal and isoprenoid alkanes, as well as a small quantity of cyclic alkanes, are present. The maximum component content in the original sample corresponds to tetradecane ($C_{14}H_{30}$), followed by a gradual decrease in the abundance of hydrocarbons with longer carbon chains. The chromatograms of the transformed saturated fractions exhibit a significant increase in lighter hydrocarbons, eluting before the eighth minute – alkanes and cycloalkanes with compositions of C_{12}–C_{14}, with the maximum corresponding to tridecane ($C_{13}H_{28}$). In the post-experiment samples, the quantity of paraffin hydrocarbons with compositions of C_{15}–C_{30} remained comparable in intensity to their content in the original sample; however, the peak heights corresponding to these compounds are relatively low due to the increased abundance of C_{12}–C_{14} components.

In the sample with sodium nanoparticles at a treatment temperature of 150 °C, compared to the control sample at 250 °C with a similar

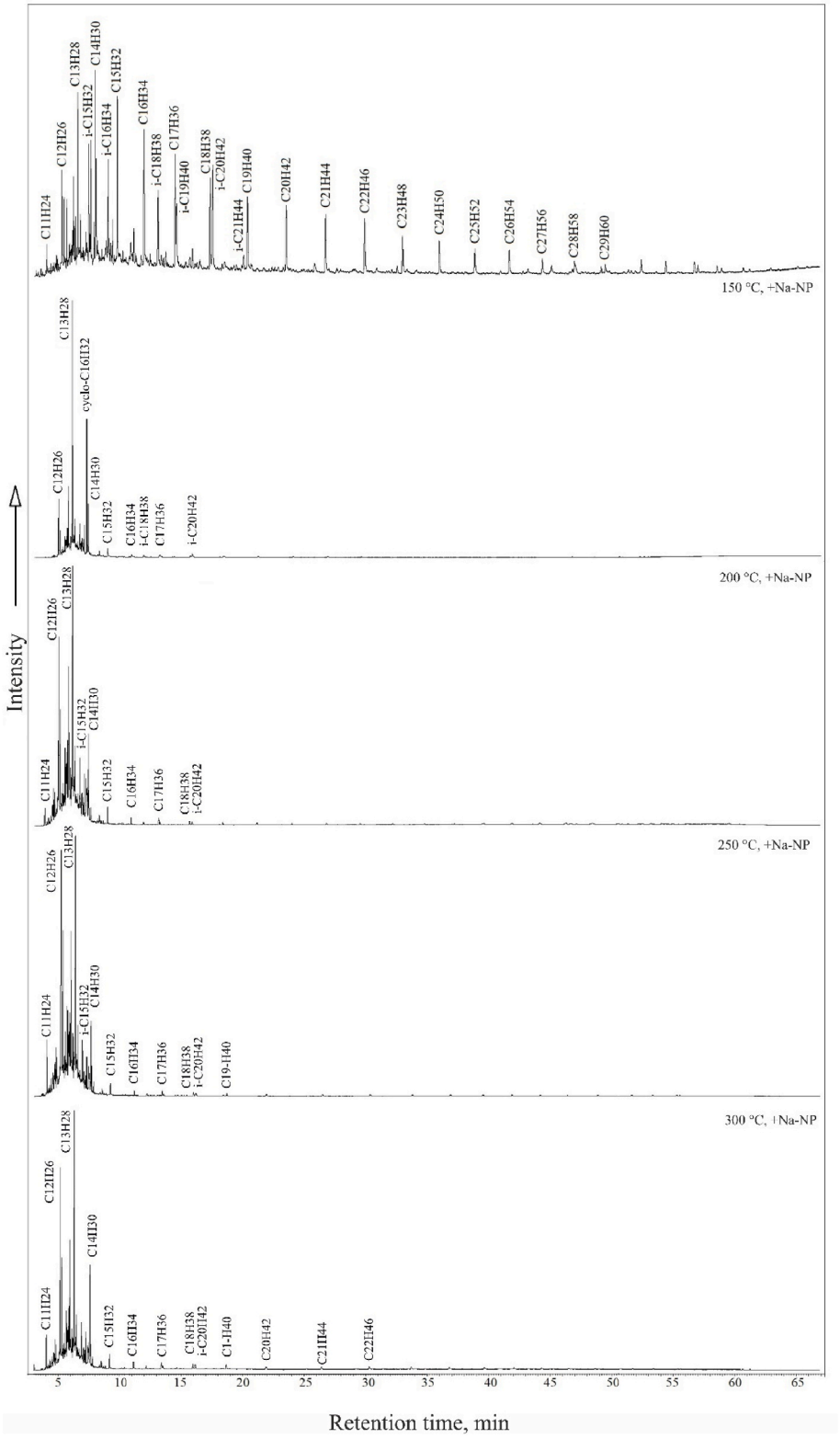

Fig. 5. Chromatograms of the saturated fraction of the studied samples.

extract yield, the content of lighter hydrocarbons with compositions of C_{10}–C_{15} is 10% higher (Fig. 6), indicating bitumoid upgrading in the presence of nanoparticles.

The highest relative content of C_{10}–C_{15} alkanes, equal to 95.74%, is observed during thermal treatment of the rock at 250 °C in the presence of a sodium nanodispersion (Fig. 6). With a subsequent increase in temperature to 300 °C, a redistribution of the alkane ratios occurs, with an increase in the proportion of C_{16}–C_{34} compounds. Evidently, in the C_{10}–C_{15} alkane molecules, C–C bond hydrogenolysis occurs, leading to the transition of low-molecular-weight hydrocarbons into the gaseous fraction, consistent with the gas chromatography data (Table 1), which registers an increase in the proportion of C_1–C_4 hydrocarbons in the gas

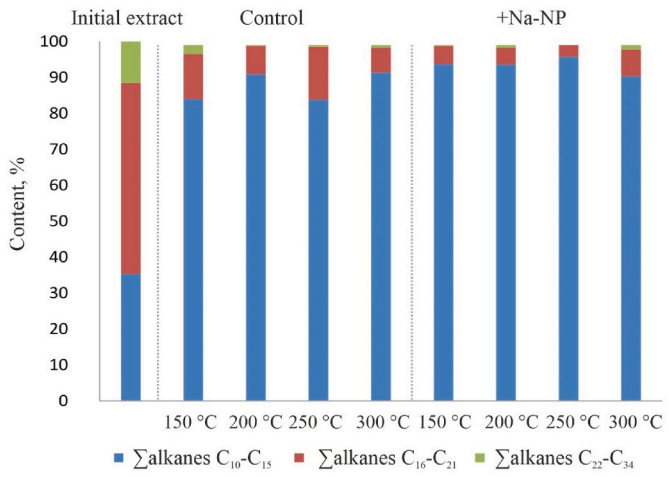

Fig. 6. Relative content of alkanes in the studied samples.

composition.

Fig. 7 shows chromatograms of the aromatic fraction (according to TIC) of the studied samples.

The chromatograms of the samples after the experiments exhibit significant differences compared to the chromatogram of the original bitumoid. While the original sample predominantly contained alkylbenzenes and alkylbenzothiophenes, the chromatograms of the transformed aromatic fractions display an increase in peaks corresponding to alkylnaphthalenes and alkyltetrahydronaphthalenes (alkyltetralins). Furthermore, in all experiments involving metallic sodium treatment, an enhancement in the peaks corresponding to naphthalenic and phenanthrenic hydrocarbons is observed, accompanied by an increase in the content of alkyldiphenyls. These observations suggest the occurrence of destructive processes involving the aromatic fragments derived from high-molecular-weight organic matter components, including kerogen.

Furthermore, during steam-thermal treatment, the content of sulfur-containing compounds – alkylbenzothiophenes, dibenzo- and naphthothiophenes – is significantly reduced (Fig. 8). However, it is necessary to consider, as evident from Fig. 4, the substantial contribution of synthetic oil to the fractional distribution of the extracted organic matter. The decrease in the proportion of sulfur-containing aromatic hydrocarbons in the control sample may only occur due to the increased proportion of synthetic oil, which exhibits a distinct fractional composition compared to the original sample. Concurrently, fluctuations in content with increasing temperature could be a consequence of changes in the composition of the additionally extracted organic matter. Alongside this, the addition of sodium nanoparticles during steam-thermal treatment facilitates near-complete desulfurization of the aromatic fraction (Fig. 8), which cannot be solely attributed to the increased proportion of synthetic oil in the sample of extracted substance. According to literature sources (De et al., 2021), metallic sodium is known to interact with aromatic sulfur-containing compounds, forming bifunctional compounds that adsorb on the surface of the rock. The use of sodium in nanoparticle form is expected to intensify this process due to the increased surface area of contact. Notably, in the case of dibenzothiophene, a compound belonging to this class, the removal of sulfur from the molecule occurs without the loss of the hydrocarbon radical (De et al., 2021). The appearance and increase of compounds with phenanthrene and hydrophenanthrene structures in the aromatic fraction at treatment temperatures of 250 °C and 300 °C can occur due to the transformation of the resin fraction in the extracted bitumen, as shown in Table 2, where their amount decreases. It is worth noting that the main contribution to the growth of the phenanthrene and hydrophenanthrene content in the aromatic fraction is made by hydrophenanthrenes, which form through the hydrogenation of phenanthrenes by active hydrogen released during the interaction of sodium with water. However, synthesizing the results of the SARA analysis (Table 2) and the distribution of compounds in the aromatic fraction (Fig. 8), it is necessary to highlight that with the use of sodium nanoparticles, a portion of the transformed aromatic hydrocarbons undergoes migration to other fractions, which becomes particularly noticeable at temperatures starting from 200 °C. Additionally, under the experimental conditions, following the interaction of sodium with water, one of the reaction products is an alkali, which is capable of actively interacting with sulfur-containing compounds, serving as an additional factor contributing to their removal. The evolved hydrogen sulfide subsequently reacts with the same sodium hydroxide, as evidenced by its absence in the gases (Table 1), forming sodium sulfide, which transitions into the aqueous phase.

The issue of sulfur removal from crude oil and petroleum products is highly relevant for a variety of reasons (Duarte et al., 2011; Shang et al., 2013; Mohebali and Ball, 2016). In this study, particular attention has been devoted to this aspect: in addition to the aforementioned indicators of the removal of sulfur-containing substances from the aromatic hydrocarbon fraction during steam-thermal treatment in the presence of sodium nanoparticles, we conducted an investigation of the total sulfur content in the extracted and treated organic matter samples using an energy-dispersive X-ray fluorescence spectrometer (Spectroscan SUL). The results demonstrated a significant reduction in sulfur content from 6.53 to 7.97 wt% in the original and control (at 250 °C) samples, respectively, to 2.69 wt% in the oil subjected to steam-thermal treatment at 250 °C in the presence of metallic sodium nanoparticles.

The degree of structural transformation of the resin-asphaltenic constituents of the extracts before and after the autoclave experiments was evaluated by Fourier-transform infrared (FTIR) spectroscopy. The structural group composition of the resin-asphaltenic substances (RAS) was determined based on the intensity of characteristic absorption bands in the IR spectra (Figs. 9 and 10, A2-A5), and the optical densities of the absorption bands were used to calculate the spectral coefficients (Tables 3 and 4): Car = D_{1600}/D_{720} (aromaticity); Cox = D_{1710}/D_{1465} (oxidation); Cbr = D_{1380}/D_{1465} (branching); Cal=$(D_{720}+D_{1380})/D_{1600}$ (aliphaticity); Csul = D_{1030}/D_{1465} (sulfur content).

Infrared spectroscopy data indicate that hydrothermal exposure to rock leads to a reduction in the content of alkyl CH_3 and CH_2 groups. This effect is particularly noticeable in asphaltenes, as evidenced by the decreased height of the absorption band peaks at 1465 cm^{-1} (Figs. 9 and 10). The spectra of transformed resins reveal that steam thermal impact on the rock in control samples does not affect the content of alkyl groups. However, the addition of sodium nanoparticles significantly reduces their presence. Furthermore, after hydrothermal treatment in the presence of sodium nanoparticles, as mentioned earlier, there is a reduction in sulfur-containing components. This reduction manifests as a decrease in the content of sulfonic groups (1420-1000 cm^{-1}) with an increase in treatment temperature and sulfoxide groups S═O (1225-980 cm^{-1}) in the resins after hydrothermal processing with metallic sodium nanoparticles.

A comparison of the spectral coefficients of the resinous-asphaltene fractions of experimental products and the original bitumoid indicates an increase in the degree of aromaticity in their structure upon hydrothermal treatment. This is evidenced by the increase in the Car coefficient values. The aliphaticity coefficient, as expected, decreased since it represents the percentage content of aliphatic fragments relative to aromatic structures and is inversely proportional to the aromaticity coefficient. The increase in the oxidation coefficient signifies a rise in the content of carbonyl groups C═O in the transformed resins and asphaltenes. The branching coefficient, which characterizes the structure of paraffin chains, changes insignificantly overall, but it noticeably decreases in asphaltenes after hydrothermal treatment in the presence of sodium nanoparticles.

Therefore, according to infrared spectroscopy data, in the transformed resins and asphaltenes, there is an increase in the content of highly condensed aromatic fragments and a decrease in aliphatic

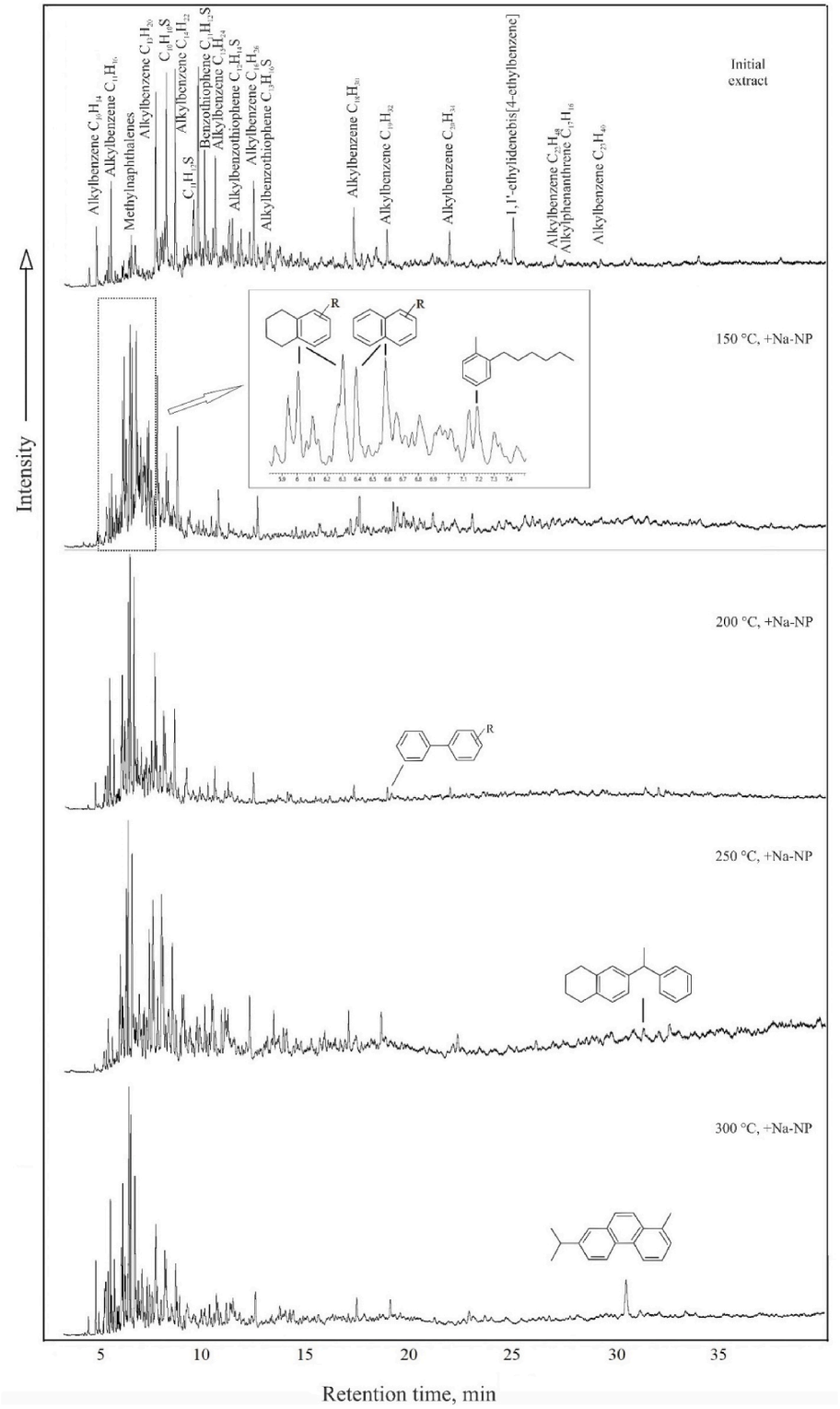

Fig. 7. Chromatograms of the aromatic fraction of the studied samples.

structures. In asphaltenes, after experiments with the application of sodium nanoparticles, there is a reduction in their degree of branching. The denser packing of aromatic rings in the structure of the resinous-asphaltene components of the experimental products results from the intensive decomposition of the kerogen structure, leading to the formation of large asphaltene-like products with subsequent detachment of alkyl chains. It is known that the degradation of kerogen is a staged process: at the first stage, heteroatomic high-molecular organic compounds are formed, from which hydrocarbon components are released upon secondary degradation (Behar et al., 2008, 2010). The reduction in the branching coefficient in asphaltenes after experiments with metallic sodium is likely associated with the detachment of alkyl chains from condensed structures and their subsequent transition to saturated hydrocarbons. This finding is corroborated by the study of SARA analysis data (Table 2).

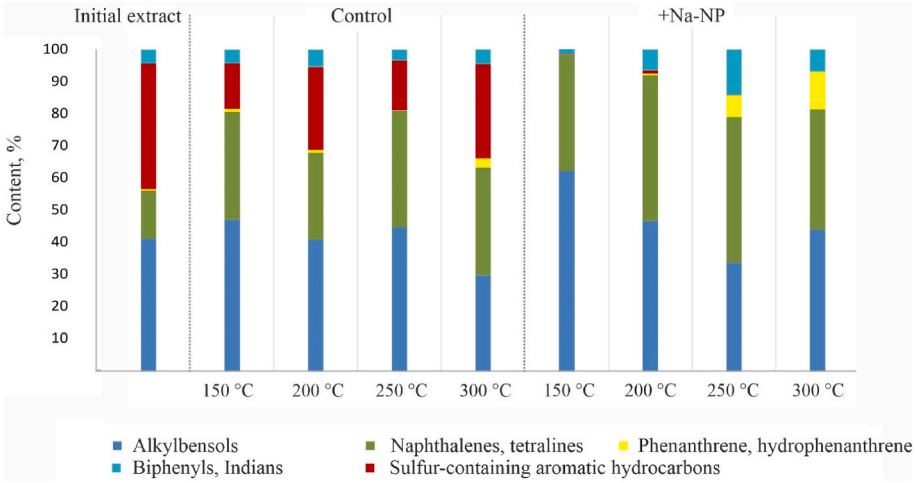

Fig. 8. Relative content of aromatic hydrocarbons in the studied samples.

Table 3
Spectral coefficients of the resin fraction.

Experiment Temperature	Spectral coefficients				
	Car	Cox	Cbr	Cal	Csul
Initial sample					
	0.60	0.22	0.78	4.00	0.78
Post thermal steam exposure					
150 °C	0.60	0.22	0.78	4.00	0.56
200 °C	0.67	0.36	0.82	3.75	0.73
250 °C	0.67	0.40	0.80	3.50	0.70
300 °C	0.63	0.45	0.82	3.40	0.91
Post thermal steam exposure in the presence of Na nanoparticles					
150 °C	0.71	0.44	0.78	2.80	0.67
200 °C	0.86	0.36	0.82	2.67	0.64
250 °C	1.00	0.75	0.88	2.17	0.75
300 °C	0.88	0.70	0.90	2.43	0.90

Table 4
Spectral coefficients of the asphaltene fraction.

Experiment Temperature	Spectral coefficients				
	Car	Cox	Cbr	Cal	Csul
Initial sample					
	0.88	0.50	1.00	2.57	0.80
Post thermal steam exposure					
150 °C	0.75	0.50	1.00	2.67	0.75
200 °C	0.83	0.57	1.00	2.60	0.86
250 °C	0.83	0.71	1.00	2.60	0.71
300 °C	0.88	0.56	1.00	2.43	0.78
Post thermal steam exposure in the presence of Na nanoparticles					
150 °C	1.00	0.44	0.89	2.33	0.67
200 °C	1.00	0.50	0.88	2.17	0.75
250 °C	1.00	0.63	1.00	2.14	0.88
300 °C	1.00	0.44	0.89	2.14	0.78

3.2. The influence of sodium metal nanoparticles on the mineral composition and structure of rocks during their hydrothermal treatment

Metallic sodium, besides its active impact on organic matter, also influences the mineral components of the rock. X-ray phase analysis data show that the original rock sample contains 59% calcite, 29% quartz, 10% potassium feldspar (microcline), 1% dolomite, and 1% pyrite (Fig. 11).

The investigation of the mineral composition of rock subjected to steam-thermal treatment at various temperatures indicates a minimal effect of these processes on its composition - the composition of the rock after control experiments is comparable to that of the original rock, with the exception of mica appearing as temperatures in the experiments increase (Fig. 12).

The addition of a sodium nanodispersion during hydrothermal treatment of rocks leads to a loss of equilibrium in the system and is accompanied by a phase transition of some minerals into others. According to the analysis, rock samples subjected to steam-thermal treatment at temperatures of 200–300 °C in an alkaline environment, while predominantly containing quartz (16–22%), include up to 6% tridymite. The polymorphic transformation into tridymite is related to changes in the crystal structure of quartz and is determined by the presence of very small amounts of certain impurities or mineralizers, primarily alkaline ions (Holmquist, 1961). This transformation is accompanied by changes in the volume of the crystal lattice and a decrease in the mineral's density, which may cause the occurrence of micro-strains in the rock.

Pyrite is identified in the composition of the original rock. Pyrite, being the most common sulfide mineral in the Earth's crust found in various genetic types of deposits, its association with carbonates and organic matter is quite common (Ma et al., 2023). XRF data suggest that as a result of hydrothermal treatment of the rock at temperatures of 200–300 °C in the presence of sodium nanodispersion, pyrite transforms into hematite—the highest oxide state of iron, a chemically more stable mineral in thermal processes. Hematite in a finely dispersed mass has hardness less than one, indicating practically no cohesion between individual particles (Li et al., 2017).

Upon steam-thermal impact at 150 °C in the presence of metallic sodium, the monoclinic modification of tobermorite – clinotobermorite - is detected on the X-ray spectrum. According to Mitsuda et al. (1992), tobermorite can form under specific conditions during autoclave treatment with steam of lime-silica mixtures in the presence of alkaline ions in the liquid phase.

The analysis of rock samples subjected to hydrothermal treatment at temperatures of 150–250 °C in the presence of sodium nanodispersion revealed the presence of boehmite and zeolite, which is presumably related to metasomatic replacement processes and hydrolysis of microcline under the influence of temperature, pressure, pH, environment chemistry, etc. Boehmite, an aluminum hydroxide, is one of the main alumina-bearing minerals of bauxites, usually dispersed and found in weakly crystalline or cryptocrystalline form. Zeolites are hydrated aluminosilicates, mainly of Ca and Na. Compared to anhydrous aluminosilicates like microcline, zeolite group minerals are characterized by lower hardness, lower specific gravity, lower refractive indices, and are more easily decomposed by acids (Król and Florek, 2022).

Therefore, hydrothermal treatment of rock in the presence of sodium nanoparticles is accompanied by structural (transition of quartz to tridymite) and phase (transformation of pyrite into hematite, etc.) changes

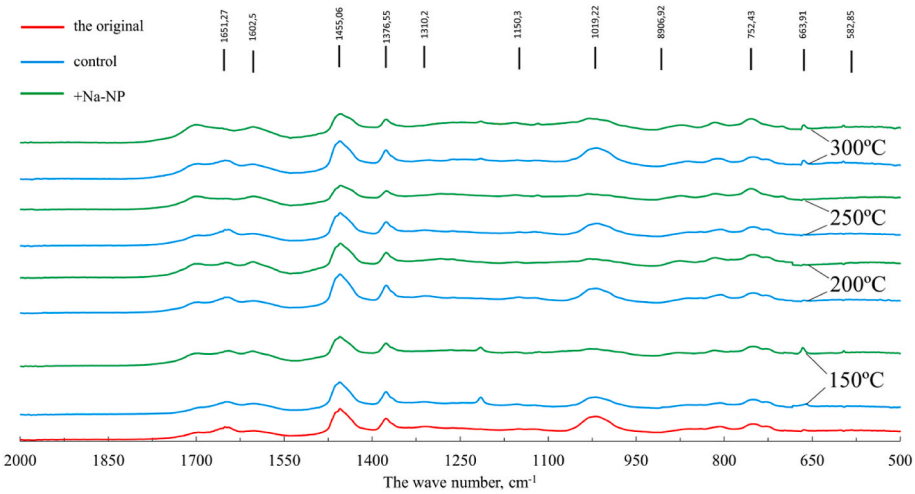

Fig. 9. IR spectra of the resin fraction of the studied samples.

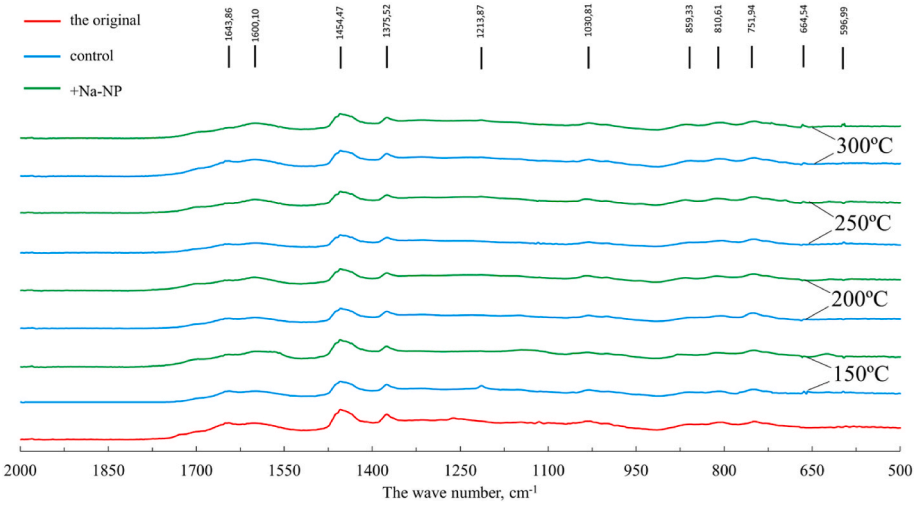

Fig. 10. IR spectra of the asphaltenes fraction of the studied samples.

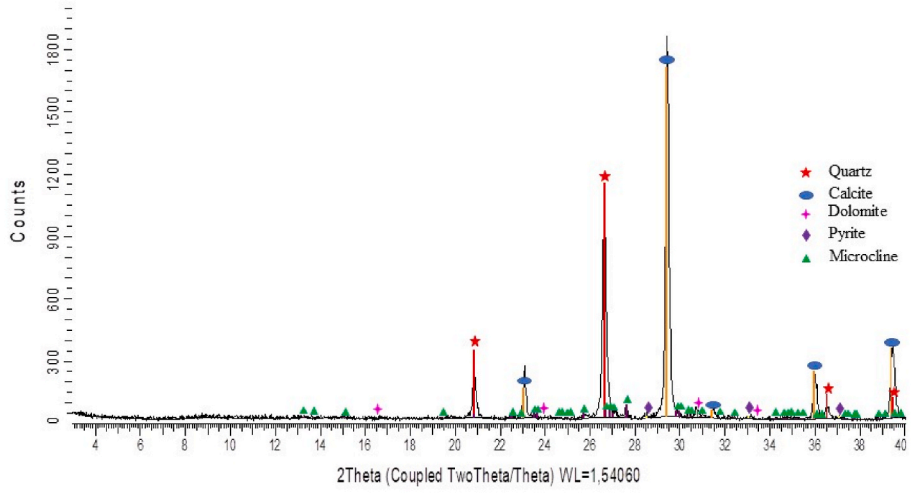

Fig. 11. X-ray diffraction pattern of a rock sample from the Domanic deposits of the Ashalcha Field.

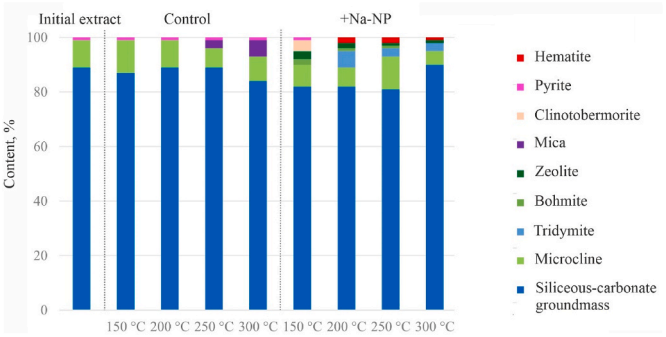

Fig. 12. Mineral composition of the rock at different experimental temperatures in the presence of sodium nanodispersion and without it.

in mineral components. Besides, the structure of kerogen contained in the rock is altered. The described changes in mineral components and kerogen could significantly affect the filtration-capacity properties of the Domanic deposits, as the void space of the rocks is transformed after each heating stage by forming new voids and channels that connect existing pores. This was shown in the work of Gilyazetdinova et al. (Giliazetdinova and Korost, 2017) who examined the transformation of void space in Domanic deposits of the South Tatar Arch during the simulation of hydrocarbon fluid generation.

4. Conclusions

Thus, the use of an organodispersion of metallic sodium nanoparticles in the hydrothermal treatment of formations with hard-to-recover reserves, including high-carbon, low-permeability rocks of Domanic formations and their analogs, is a promising method for enhancing oil flow and increasing overall reservoir recovery. This method can be recommended for application on a pilot scale. Beyond the evident advantages of using sodium in thermal extraction methods, which, upon interaction with water, generates additional heat, fosters the formation of gaseous hydrogen and active alkali, it positively influences the processes in oil extraction. Specifically, in the presence of sodium nanoparticles in the reaction system, the processes of kerogen destruction and high-molecular heteroatomic compounds of resinous-asphaltene substances are intensified, leading to the formation of free hydrocarbons, thereby facilitating their more complete extraction from the rock. In the group composition of extracts, the proportion of saturated hydrocarbons increases while the resinous-asphaltene substances decrease. A significant rise in the proportion of lighter hydrocarbons is observed in the saturated fraction. The addition of sodium nanoparticles during steam-thermal treatment nearly entirely removes sulfur from the aromatic fraction. The overall sulfur content in the extracts also significantly decreases from 6.53 to 7.97 wt% in the original and control (at 250 °C) samples respectively, to 2.69 wt% in the presence of metallic sodium. Subsequently, the sodium hydroxide formed after the interaction of sodium with water reacts with the released hydrogen sulfide and carbon dioxide, forming sodium sulfide and sodium carbonate, respectively, which are removed in the aqueous phase, as evidenced by the absence of H_2S and CO_2 in the gases.

The most optimal condition for hydrothermal treatment using sodium nanoparticles was found to be a reaction temperature of 250 °C, with further increases in treatment temperature leading to the loss of liquid hydrocarbons due to intense gas formation. It is also noteworthy that the addition of sodium nanodispersion offers the advantage of lowering the steam-thermal treatment temperature by 100 °C while maintaining a similar capacity for extracting organic matter.

Hydrothermal treatment of rock in the presence of sodium nanoparticles results in structural and phase transformations of mineral components, accompanied by changes in the volume and density of the rock. In addition, the structural composition of kerogen contained in the rock changes. The combination of these factors leads to the transformation of the void space in the rock and affects the filtration capacity properties of reservoirs.

For a more comprehensive understanding of the transformation of the void space in low-permeability high-carbon Domanic deposits and the conversion of sulfur-containing components of the extracted organic matter during hydrothermal treatment in the presence of sodium nanoparticles, further research becomes a necessity.

Conflict of interest

The authors declare no competing financial interest.

CRediT authorship contribution statement

Liliya Kh Galiakhmetova: Writing – original draft, Methodology, Investigation, Formal analysis, Data curation. **Aydar A. Kayumov:** Data curation, Investigation, Writing – review & editing. **Vladimir E. Katnov:** Writing – original draft, Validation, Supervision, Methodology, Investigation, Formal analysis, Data curation, Conceptualization. **Mohammed A. Khelkhal:** Writing – review & editing, Writing – original draft, Visualization, Validation, Formal analysis, Data curation. **Rezeda E. Mukhamatdinova:** Formal analysis, Data curation. **Sofya A. Trubitsina:** Investigation, Formal analysis, Data curation. **Nafis A. Nazimov:** Investigation, Formal analysis. **Alexey V. Vakhin:** Validation, Supervision, Project administration, Funding acquisition.

Declaration of competing interest

The authors declare that they have no known competing financial interests or personal relationships that could have appeared to influence the work reported in this paper.

Data availability

Data will be made available on request.

Acknowledgment

This work was supported by the Russian Science Foundation (grant no. 23-73-10170).

Appendix 1

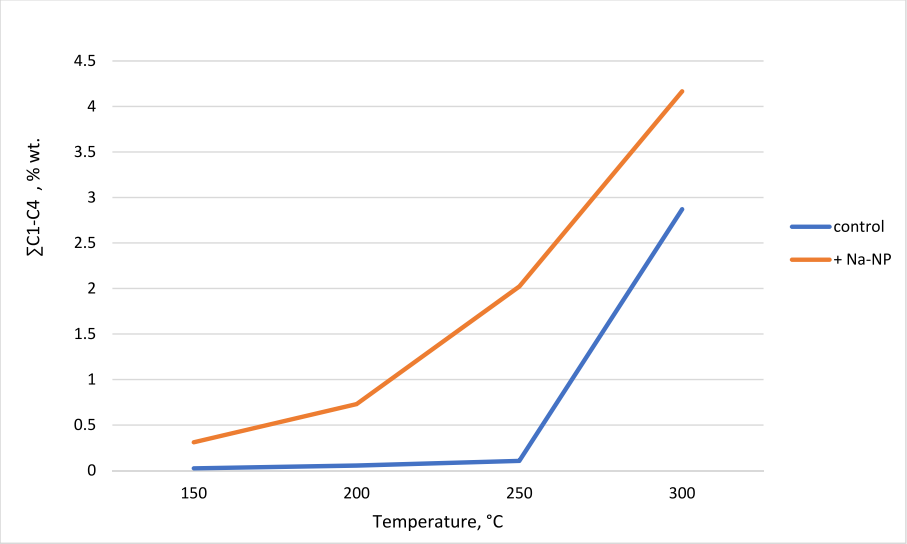

Figure A1. Temperature dependence of the yield of hydrocarbon gases during thermal steam treatment of Domanic rock.

References

Aadnøy, B.S., Looyeh, R., 2019. Shale oil, shale gas, and hydraulic fracturing. Pet. Rock mech. https://doi.org/10.1016/b978-0-12-815903-3.00016-9.

Agrawal, V., Sharma, S., 2018. Improved kerogen models for determining thermal maturity and hydrocarbon potential of shale. Sci. Rep. 8 https://doi.org/10.1038/s41598-018-35560-8.

Aguilera, R.F., Eggert, R.G., Lagos, C.C.G., Tilton, J.E., 2009. Depletion and the future availability of petroleum resources. Energy J. 30 https://doi.org/10.5547/ISSN0195-6574-EJ-Vol30-No1-6.

Al-Mishaal, O.F., Suwaid, M.A., Al-Muntaser, A.A., Khelkhal, M.A., Varfolomeev, M.A., Djimasbe, R., et al., 2022. Octahedral cluster complex of molybdenum as oil-soluble catalyst for improving in situ upgrading of heavy crude oil: synthesis and Application. Catalysts 12, 1125. https://doi.org/10.3390/catal12101125.

Aliev, F.A., Mukhamatdinov, I.I., Sitnov, S.A., Ziganshina, M.R., Onishchenko, Y.V., Sharifullin, A.V., et al., 2021. In-situ heavy oil aquathermolysis in the presence of nanodispersed catalysts based on transition metals. Processes 9, 127. https://doi.org/10.3390/pr9010127.

Alomair, O.A., Matar, K.M., Alsaeed, Y.H., 2014. Nanofluids application for heavy oil recovery. Soc. Pet. Eng. - SPE Asia Pacific oil gas Conf. Exhib. APOGCE 2014 - Chang. Game oppor. Challenges Solut. 2 https://doi.org/10.2118/171539-ms.

Behar, F., Lorant, F., Lewan, M., 2008. Role of NSO compounds during primary cracking of a Type II kerogen and a Type III lignite. Org. Geochem. 39 https://doi.org/10.1016/j.orggeochem.2007.10.007.

Behar, F., Roy, S., Jarvie, D., 2010. Artificial maturation of a Type I kerogen in closed system: mass balance and kinetic modelling. Org. Geochem. 41 https://doi.org/10.1016/j.orggeochem.2010.08.005.

Bychkov, A.Y., Kalmykov, G.A., Bugaev, I.A., 2015. Experimental studies of the production of hydrocarbon fluids from rocks of the Bazhenov formation under hydrothermal conditions. Moscow Univ. Geol. Bull. 34–39.

Clark, P.D., Hyne, J.B., Tyrer, J.D., 1983. Chemistry of organosulphur compound types occurring in heavy oil sands. Fuel 62, 959–962. https://doi.org/10.1016/0016-2361(83)90170-9.

De, P.B., Asako, S., Ilies, L., 2021. Recent advances in the use of sodium dispersion for organic synthesis. Synth. Met. 53 https://doi.org/10.1055/a-1478-7061.

Duarte, F.A., Mello, P.D.A., Bizzi, C.A., Nunes, M.A.G., Moreira, E.M., Alencar, M.S., et al., 2011. Sulfur removal from hydrotreated petroleum fractions using ultrasound-assisted oxidative desulfurization process. Fuel 90. https://doi.org/10.1016/j.fuel.2011.01.030.

Fallis, A., 2013. Handbook of Petroleum Product Analysis, 53.

Foda, S., 2015. Refracturing: technology and reservoir understanding are giving new life to depleted unconventional assets. JPT, J Pet Technol 67. https://doi.org/10.2118/0715-0076-jpt.

Gabrielsen, R.H., 2010. The structure and hydrocarbon traps of sedimentary basins. Pet. Geosci. From Sediment. Environ. to Rock Phys. https://doi.org/10.1007/978-3-642-02332-3_12.

Galukhin, A., Nosov, R., Eskin, A., Khelkhal, M., Osin, Y., 2019. Manganese oxide nanoparticles immobilized on silica nanospheres as a highly efficient catalyst for heavy oil oxidation. Ind. Eng. Chem. Res. 58, 8990–8995. https://doi.org/10.1021/acs.iecr.9b00080.

Giliazetdinova, D., Korost, D., 2017. Studying of shale organic matter structure and pore space transformations during hydrocarbon generation. Adv. Lab. Test. Model 382–387. https://doi.org/10.1007/978-3-319-52773-4_45. Soils Shales, Springer.

Gordadze, G.N., Giruts, M.V., Koshelev, V.N., 2010. Petroleum Hydrocarbons and Their Analysis by Gas Chromatography.

Gray, M.R., 2019. Fundamentals of partial upgrading of bitumen. Energy Fuel. 33 https://doi.org/10.1021/acs.energyfuels.9b01622.

Holmquist, Sb, 1961. Conversion of quartz to tridymite. J. Am. Ceram. Soc. 44 https://doi.org/10.1111/j.1151-2916.1961.tb15355.x.

Ibatullin, R.R., 2017. Experience in north America tight oil reserves development. Horizontal wells and multistage hydraulic fracturing. Georesursy 19. https://doi.org/10.18599/grs.19.3.4.

Kalmykov, A.G., Bychkov, A.Y., Kalmykov, G.A., Bugaev, I.A., Kozlova, E.V., 2017. Generation potential of kerogen of the bazhenov formation and possibility of its implementation. Georesursy 19. https://doi.org/10.18599/grs.19.17.

Karpov, I.K., Zubkov, V.S., Stepanov, A.N., Bychinskii, V.A., Artimenko, M.V., 1998. A thermodynamic criterion of metastable state of hydrocarbons in the Earth's crust and upper mantle. Geol i Geofiz.

Katnov, V.E., Trubitsina, S.A., Kayumov, A.A., Aliev, F.A., Nazimov, N.A., Dengaev, A.V., et al., 2023. Influence of sodium metal nanoparticles on the efficiency of heavy oil aquathermolysis. Catalysts 13. https://doi.org/10.3390/catal13030609.

Kayukova, G.P., Kiyamova, A.M., Mikhailova, A.N., Kosachev, I.P., Petrov, S.M., Romanov, G.V., et al., 2016. Generation of hydrocarbons by hydrothermal transformation of organic matter of domanik rocks. Chem. Technol. Fuels Oils 52, 149–161. https://doi.org/10.1007/s10553-016-0685-2.

Kayukova, G.P., Mikhailova, A.N., Kosachev, I.P., Eskin, A.A., Morozov, V.I., 2019. Effect of the natural minerals pyrite and hematite on the transformation of Domanik Rock organic matter in hydrothermal processes. Pet Chem 59. https://doi.org/10.1134/S0965544119010080.

Kayukova, G.P., Mikhailov, A.N., Kosachev, I.P., Morozov, V.P., Vakhin, A.V., 2020. Hydrothermal transformations of organic matter of Carbon-Rich Domanik Rock in Carbon dioxide environment at different temperatures. Pet Chem 60. https://doi.org/10.1134/S0965544120030093.

Kosachev, I.P., Borisov, D.N., Milordov, D.V., Mironov, N.A., Yakubova, S.G., Yakubov, M.R., et al., 2022. Changes in the composition of heavy oil during thermolysis in the presence of molten sodium without hydrogen. Energy Sources, Part A Recover Util. Environ Eff 44. https://doi.org/10.1080/15567036.2019.1654561.

Kravchenko, M.N., Dmitriev, N.M., Muraduv, A.V., Dieva, N.N., Gerasimov, V.V., 2016. Innovative development methods of Kerogen-Bearing reservoirs that promote oil generating potential. Georesursy= Georesources 18, 330–336. https://doi.org/10.18599/grs.18.4.12.

Kravchenko, M.N., Dieva, N.N., Lishchuk, A.N., Muradov, A.V., Vershinin, V.E., 2018. Hydrodynamic modeling of thermochemical treatment of low permeable kerogen-containing reservoirs. Georesursy 20. https://doi.org/10.18599/grs.2018.3.178-185.

Król, M., Florek, P., 2022. Zeolites. MDPI-Multidisciplinary Digital Publishing Institute.

Kruse, A., Dinjus, E., 2007. Hot compressed water as reaction medium and reactant. J. Supercrit. Fluids 39 (3), 362–380. https://doi.org/10.1016/j.supflu.2006.03.016.

Lakhova, A., Petrov, S., Ibragimova, D., Kayukova, G., Safiulina, A., Shinkarev, A., et al., 2017. Aquathermolysis of heavy oil using nano oxides of metals. J. Pet. Sci. Eng. 153, 385–390. https://doi.org/10.1016/J.PETROL.2017.02.015.

Lewan, M.D., 1997. Experiments on the role of water in petroleum formation. Geochim. Cosmochim. Acta 61, 3691–3723. https://doi.org/10.1016/s0016-7037(97)00176-2.

Li, D., Yin, W., Liu, Q., Cao, S., Sun, Q., Zhao, C., et al., 2017. Interactions between fine and coarse hematite particles in aqueous suspension and their implications for flotation. Miner. Eng. 114 https://doi.org/10.1016/j.mineng.2017.09.012.

Liang, M., Wang, Z., Zheng, J., Li, X., Wang, X., Gao, Z., et al., 2015. Hydrous pyrolysis of different kerogen types of source rock at high temperature-bulk results and biomarkers. J. Pet. Sci. Eng. 125 https://doi.org/10.1016/j.petrol.2014.11.021.

Liang, X., Jin, Z., Philippov, V., Obryadchikov, O., Zhong, D., Liu, Q., et al., 2020. Sedimentary characteristics and evolution of domanik facies from the Devonian–Carboniferous regression in the southern Volga-Ural basin. Mar Pet Geol 119. https://doi.org/10.1016/j.marpetgeo.2020.104438.

Ma, S., Shi, M., Zhang, C., Cao, Q., 2023. Mineralogical characteristics and genetic types of pyrite with different occurrence: Constraints from spectroscopy, Geochemistry and δ34S stable Isotopes. Minerals 14, 52. https://doi.org/10.3390/min14010052.

Maghzi, A., Mohammadi, S., Ghazanfari, M.H., Kharrat, R., Masihi, M., 2012. Monitoring wettability alteration by silica nanoparticles during water flooding to heavy oils in five-spot systems: a pore-level investigation. Exp. Therm. Fluid Sci. 40 https://doi.org/10.1016/j.expthermflusci.2012.03.004.

Mikhailova, A.N., Kayukova, G.P., Batalin, G.A., Babayev, V.M., Vakhin, A.V., 2020. Comparative influence's research of the compound of metals carboxylates on the generation and composition of hydrocarbons from Domanic deposits at steam-thermal effect in CO_2 environment. J. Pet. Sci. Eng. 186 https://doi.org/10.1016/j.petrol.2019.106699.

Mitsuda, T., Sasaki, K., Ishida, H., 1992. Phase evolution during autoclaving process of aerated concrete. J. Am. Ceram. Soc. 75, 1858–1863. https://doi.org/10.1111/j.1151-2916.1992.tb07208.x.

Mohebali, G., Ball, A.S., 2016. Biodesulfurization of diesel fuels - Past, present and future perspectives. Int. Biodeterior. Biodegrad. 110 https://doi.org/10.1016/j.ibiod.2016.03.011.

Morozov, V.P., Khayuzkin, A.S., Korolev, E.A., Kolchugin, A.N., Mukhamediyarova, A.N., Morozova, E.V., et al., 2022. Geological prerequisites for the search for rocks with increased reservoir properties in domanic type sediments on the territory of the Republic of Tatarstan. Georesursy 24. https://doi.org/10.18599/grs.2022.4.3.

Nasyrova, Z.R., Kayukova, G.P., Khasanova, N.M., Vakhin, A.V., 2020a. Transformation of organic matter of domanik rock from the Romashkino Oilfield in sub- and supercritical water. Pet Chem 60. https://doi.org/10.1134/S0965544120060079.

Nasyrova, Z.R., Kayukova, G.P., Vakhin, A.V., Djimasbe, R., Chemodanov, A.E., 2020b. Heavy oil hydrocarbons and kerogen destruction of carbonate–siliceous domanic shale rock in sub-and supercritical water. Processes 8, 800. https://doi.org/10.3390/pr8070800.

Nasyrova, Z.R., Kayukova, G.P., Vakhin, A.V., Gareev, B.I., Eskin, A.A., 2021. Transformation of Carbon-rich organic components of a Domanik rock in Sub- and Supercritical aqueous fluids. Pet Chem 61. https://doi.org/10.1134/S0965544121060062.

Nasyrova, Z.R., Kayukova, G.P., Vakhin, A.V., Shmeleva, E.I., Mukhamedyarova, A.N., Khasanova, N.M., et al., 2022. Transformation of the organic matter of low-permeability domanik rock in supercritical water and 1-propanol (A review). Pet Chem 62. https://doi.org/10.1134/S096554412201008X.

Onishchenko, Y.V., Vakhin, A.V., Gareev, B.I., Batalin, G.A., Morozov, V.P., Eskin, A.A., 2019. The material balance of organic matter of Domanic shale formation after thermal treatment. Pet Sci Technol 37, 756–762. https://doi.org/10.1080/10916466.2018.1558247.

Ross, D.S., Nguyen, Q., 1983. Coal Conversion in Aqueous Systems//Fluid Phase Equilibria, 10, pp. 319–326.

Shang, H., Zhang, H., Du, W., Liu, Z., 2013. Development of microwave assisted oxidative desulfurization of petroleum oils: a review. J. Ind. Eng. Chem. 19 https://doi.org/10.1016/j.jiec.2013.01.015.

Shayan Nasr, M., Esmaeilnezhad, E., Choi, H.J., 2021. Effect of carbon-based and metal-based nanoparticles on enhanced oil recovery: a review. J. Mol. Liq. 338 https://doi.org/10.1016/j.molliq.2021.116903.

Sitnov, S.A., Mukhamatdinov, I.I., Shmeleva, E.I., Aliev, F.A., Vakhin, A.V., 2019. Influence of nanosized iron oxides (II, III) on conversion of biodegradated oil. Pet Sci Technol 37, 971–976. https://doi.org/10.1080/10916466.2019.1575872.

Sun, X., Zhang, Y., Chen, G., Gai, Z., 2017. Application of nanoparticles in enhanced oil recovery: a critical review of recent progress. Energies 10. https://doi.org/10.3390/en10030345.

Tajik, A., Farhadian, A., Khelkhal, M.A., Rezaeisadat, M., Petrov, S.M., Eskin, A.A., et al., 2023. Sunflower oil as renewable biomass source to develop highly effective oil-soluble catalysts for in-situ combustion of heavy oil. Chem Eng J 453, 139813. https://doi.org/10.1016/j.cej.2022.139813.

Tang, J., Kye, D.K., Pol, V.G., 2018. Ultrasound-assisted synthesis of sodium powder as electrode additive to improve cycling performance of sodium-ion batteries. J. Power Sources 396. https://doi.org/10.1016/j.jpowsour.2018.06.067.

Tumanyan, B.P., Petrukhina, N.N., Kayukova, G.P., Nurgaliev, D.K., Foss, L.E., Romanov, G.V., 2015. Aquathermolysis of crude oils and natural bitumen: chemistry, catalysts and prospects for industrial implementation. Russ. Chem. Rev. 84, 1145–1175. https://doi.org/10.1070/RCR4500.

Vakhin, A.V., Onishchenko, Y.V., Ostolopovskaya, O.V., Khelkhal, M.A., 2024. Unraveling thermal maturation and hydrocarbon generation in domanic oil shale through integrated physicochemical analysis. Energy Fuel. 38, 1173–1180. https://doi.org/10.1021/acs.energyfuels.3c04059.

Vandenbroucke, M., 2003. Kerogan: from types to models of chemical structure. Oil Gas Sci. Technol. 58 https://doi.org/10.2516/ogst:2003016.

Zhang, L.X., Liu, Y.Z., 2001. Properties, preparation and application of ultrafine powder. Huabei Gongxueyuan Xuebao/Journal North China Inst Technol 22. https://doi.org/10.1142/9789812386588_0003.

Zhang, Z., Volkman, J.K., Greenwood, P.F., Hu, W., Qin, J., Borjigin, T., et al., 2014. Flash pyrolysis of kerogens from algal rich oil shales from the Eocene Huadian Formation, NE China. Org. Geochem. 76 https://doi.org/10.1016/j.orggeochem.2014.08.004.

Zhao, F., Liu, Y., Wu, Y., Zhao, X., Tan, L., 2012. Study of catalytic aquathermolysis of heavy oil in the presence of a hydrogen donor. Chem. Technol. Fuels Oils 48, 273–282. https://doi.org/10.1007/s10553-012-0368-6.

Zou, C., Zhao, Q., Zhang, G., Xiong, B., 2016. Energy revolution: from a fossil energy era to a new energy era. Nat. Gas. Ind. B 3. https://doi.org/10.1016/j.ngib.2016.02.001.